Am J Physiol Regul Integr Comp Physiol 293: R1159–R1168, 2007.
First published June 20, 2007; doi:10.1152/ajpregu.00767.2006.

Denervation-induced skeletal muscle atrophy is associated with increased mitochondrial ROS production

Florian L. Muller,[2] Wook Song,[2] Youngmok C. Jang,[2] Yuhong Liu,[2] Marian Sabia,[1] Arlan Richardson,[1,2,3] and Holly Van Remmen[1,2,3]

[1]*South Texas Veterans Health Care System, San Antonio; and* [2]*Department of Cellular and Structural Biology and* [3]*Barshop Institute for Longevity and Aging Studies, University of Texas Health Science Center at San Antonio, San Antonio, Texas*

Submitted 3 November 2006; accepted in final form 19 June 2007

Muller FL, Song W, Jang YC, Liu Y, Sabia M, Richardson A, Van Remmen H. Denervation-induced skeletal muscle atrophy is associated with increased mitochondrial ROS production. *Am J Physiol Regul Integr Comp Physiol* 293: R1159–R1168, 2007. First published June 20, 2007; doi:10.1152/ajpregu.00767.2006.—Reactive oxygen species (ROS), especially mitochondrial ROS, are postulated to play a significant role in muscle atrophy. We report a dramatic increase in mitochondrial ROS generation in three conditions associated with muscle atrophy: in aging, in mice lacking CuZn-SOD (*Sod1*$^{-/-}$), and in the neurodegenerative disease, amyotrophic lateral sclerosis (ALS). ROS generation in muscle mitochondria is nearly threefold higher in 28- to 32-mo-old than in 10-mo-old mice and is associated with a 30% loss in gastrocnemius mass. In *Sod1*$^{-/-}$ mice, muscle mitochondrial ROS production is increased >100% in 20-mo compared with 5-mo-old mice along with a >50% loss in muscle mass. ALS G93A mutant mice show a 75% loss of muscle mass during disease progression and up to 12-fold higher muscle mitochondrial ROS generation. In a second ALS mutant model, H46RH48Q mice, ROS production is approximately fourfold higher than in control mice and is associated with a less dramatic loss (30%) in muscle mass. Thus ROS production is strongly correlated with the extent of muscle atrophy in these models. Because each of the models of muscle atrophy studied are associated to some degree with a loss of innervation, we were interested in determining whether denervation plays a role in ROS generation in muscle mitochondria isolated from hindlimb muscle following surgical sciatic nerve transection. Seven days postdenervation, muscle mitochondrial ROS production increased nearly 30-fold. We conclude that enhanced generation of mitochondrial ROS may be a common factor in the mechanism underlying denervation-induced atrophy.

mitochondria; reactive oxygen species; amyotrophic lateral sclerosis; copper, zinc superoxide dismutase

SKELETAL MUSCLE ATROPHY is a debilitating phenotype that is associated with a variety of conditions, including neurodegenerative diseases, cancer cachexia, and immobilization or disuse (49, 56, 76, 77). Muscle atrophy is also an unavoidable consequence of normal human aging (43, 68). Despite the importance and impact of losing muscle mass, the biochemical and molecular mechanisms leading to muscle atrophy are still poorly understood. Several potential contributing factors in loss of muscle mass have been identified, including neuromuscular alterations, changes in protein synthesis and degradation, and loss of fibers due to apoptosis (15, 52, 58). Oxidative stress and mitochondrial dysfunction have also been implicated in sarcopenia (27, 62), hindlimb unloading (3, 46, 65), and in atrophic mouse muscle from amyotrophic lateral sclerosis (ALS) transgenic mice (54). Because mitochondria are an important source of reactive oxygen species (ROS) in cells, we were interested in delineating the role of muscle mitochondrial ROS generation in muscle atrophy. In this study, we measured mitochondrial ROS production during aging in wild-type mice and in mutant mouse models associated with significant loss of muscle mass to assess the importance of ROS generation in the basic mechanism(s) underlying muscle atrophy.

The first muscle atrophy model we studied is a knockout mouse lacking a major antioxidant enzyme, CuZn-SOD [*Sod1*$^{-/-}$ mice (67)]. In a recent study, we reported that the *Sod1*$^{-/-}$ mice show a dramatic age-related loss of skeletal muscle mass that is accelerated compared with wild-type mice (57). By 20 mo of age, the *Sod1*$^{-/-}$ mice have lost nearly 50% of their hindlimb muscle mass. The loss of mass is greatest in the gastrocnemius, whereas the soleus muscle is relatively spared. This is similar to the pattern of muscle loss seen in wild-type mice during aging, since muscles with high proportions of type IIb fibers such as gastrocnemius are more susceptible to loss of mass than muscles with higher percentages of type I oxidative fibers, such as the soleus (34). The *Sod1*$^{-/-}$ mice are also characterized by very high levels of oxidative stress and elevated levels of oxidative damage to lipid, protein, and DNA in several tissues, including skeletal muscle (57).

The second type of mutant mouse model we used in this study is transgenic mice overexpressing mutant forms of CuZn-SOD that are found in humans with the neurodegenerative disease ALS. ALS is characterized by selective loss of upper and lower motor neurons, which ultimately leads to muscle atrophy, paralysis, and death from respiratory failure (61). Transgenic mice expressing mutant forms of the CuZn-SOD protein develop a disease strikingly similar to ALS (31), including paralysis and significant loss of muscle mass during the course of the disease, and are extensively used as a model to study the disease. We measured ROS production in skeletal muscle mitochondria from two different CuZn-SOD mutant mouse lines [G93A (31) and H46RH48Q (81)]. Both of these mutant mouse lines exhibit paralysis and muscle atrophy during progression of the disease but differ in the time course of disease progression and, as we report for the first time, also in the extent and pattern of loss of muscle mass. In the G93A mutant mice, the first symptoms (tremor and muscle weakness)

Address for reprint requests and other correspondence: H. Van Remmen, Dept. Cellular and Structural Biology, Univ. of Texas Health Science Center at San Antonio, Barshop Institute for Longevity and Aging Studies, 15355 Lambda Drive Mail Code 7755, San Antonio, TX 78245-3207 (e-mail: vanremmen@uthscsa.edu).

The costs of publication of this article were defrayed in part by the payment of page charges. The article must therefore be hereby marked "*advertisement*" in accordance with 18 U.S.C. Section 1734 solely to indicate this fact.

appear at ~90 days, and the disease reaches end stage, characterized by a dramatic loss of neurons (50%), at around 150 days (30). In the H46RH48Q mutant mice, the onset of the disease is later, at ~180 days of age, and the mice die at ~240 days. In contrast to the G93A mutant mice, the H46RH48Q mice do not develop significant muscle atrophy until late in the course of the disease.

In this study, we propose that mitochondrial ROS is a critical factor in the mechanism underlying muscle atrophy. In agreement with our hypothesis, in all three models we observed a significant increase in ROS generation that correlated to the extent of muscle atrophy, i.e., greater ROS generation in models exhibiting greater atrophy. Because the atrophy that occurs in the three conditions we studied (aging, *Sod1*$^{-/-}$ mice, and ALS) is largely the result of loss of innervation, we asked whether mitochondrial generation of ROS would be induced by surgical denervation. Indeed, transection of the sciatic nerve led to rapid muscle mass loss and a dramatic increase in mitochondria ROS production. Thus we have uncovered an important role for loss of innervation in the induction of skeletal muscle mitochondrial ROS generation, oxidative stress, and loss of muscle mass.

EXPERIMENTAL PROCEDURES

Animals. The *Sod1*$^{-/-}$ mice used in this study were generated by Dr. Charles Epstein's laboratory at the University of California, San Francisco and were previously described (19, 35). The mice were maintained in the heterozygous state (*Sod1*$^{+/-}$) and backcrossed with C57Bl/6J females (Jackson Laboratory, Bar Arbor, ME) for at least 12 generations. Two different ALS mouse models were employed. The widely used G93A mouse model [C57Bl/6J Tg (SOD1-G93A) 1Gur/J mice (31)] was obtained from the Jackson Laboratory. The H46RH48Q mutant mouse model [C57Bl/6J × C3H Tg (SOD1-H46RH48Q) mice (81), line 139] was kindly provided by Dr. David Borchelt (University of Florida, Gainesville, FL). All mice were maintained under specific pathogen-free conditions, and all procedures for handling animals in this study were reviewed and approved by the Institutional Animal Care and Use Committee (IACUC) of the University of Texas Health Science Center at San Antonio and the IACUC of Audie L. Murphy Memorial Veterans Hospital.

Mitochondrial isolation. Mitochondria were purified from whole hindlimb skeletal muscle (with the exception of the sciatic nerve transection experiments, in which only the gastrocnemius, soleus, and tibialis were used) according to Chappell and Perry (11, 20), as described previously (55). Hindlimb skeletal muscle was excised, weighed, bathed in 150 mM KCl, and placed in Chappell-Perry buffer with the protease nagarse. The minced skeletal muscle was homogenized, and the homogenate was centrifuged for 10 min at 600 *g*, with the supernatant then being passed through cheesecloth and centrifuged at 14,000 *g*for 10 min. The resulting pellet was washed once in modified Chappell-Perry buffer with 0.5% bovine serum albumin and once in modified Chappell-Perry buffer without bovine serum albumin. Mitochondria were used immediately. Protein concentration was measured with the Bradford method.

Mitochondrial H_2O_2 release. Mitochondrial ROS production was measured with the Amplex red-horseradish peroxidase (HRP) method (Molecular Probes, Eugene, OR) (85). HRP (2 U/ml) catalyzes the H_2O_2-dependent oxidation of nonfluorescent Amplex red (80 μM) to fluorescent resorufin red (85). CuZn-SOD (37 U/ml) was added to convert all $O_2^{\bullet-}$ into H_2O_2, a necessity since $O_2^{\bullet-}$ reacts very rapidly with HRP and HRP-compound I, resulting in underestimation of the actual rate of H_2O_2 production (5, 44). Therefore, our results reflect the sum of both superoxide and H_2O_2 production and are referred to as ROS rather than H_2O_2 production (55). Fluorescence was followed at an excitation wavelength of 545 nm and emission wavelength of 590 nm using a Fluoroskan Ascent type 374 multiwell plate reader (Labsystems, Helsinki, Finland). The slope of the increase in fluorescence is converted to the rate of H_2O_2 production with a standard curve. We performed all assays at 37°C in 96-well plates. Substrates used were 5 mM succinate and 5 mM glutamate plus malate. For each assay, one reaction well contained buffer only, and another contained buffer with mitochondria, to estimate the background oxidation rates of Amplex red and to estimate the rate of H_2O_2 release in mitochondria without substrate (state 1) (9). The reaction buffer consisted of 125 mM KCl, 10 mM HEPES, 5 mM $MgCl_2$, and 2 mM K_2HPO_4, pH 7.44.

Mitochondrial respiration. Mitochondrial oxygen consumption was measured using a Clark electrode (83) (Oxytherm; oxygen electrode system from PP System, Hansatech Instruments) as originally described by Estabrook (21). The respiratory buffer consisted of 125 mM KCl, 10 mM HEPES, 5 mM $MgCl_2$, and 2 mM K_2HPO_4, pH 7.44, with 0.3% BSA. State 3 respiration was induced with the addition of 0.3 mM ADP.

Denervation. Sciatic nerve transection (47, 79) was performed on C57BL/6J females ages 3 to 5 mo. Animals were anesthetized using constant-flow isoflurane inhalation anesthesia. In each hindlimb (at the level of the femur), a small incision was made and the sciatic nerve was isolated. In the left leg, the sciatic nerve was severed and a 5-mm section of sciatic nerve was removed. The ends of the nerve were folded back and sutured to prevent nerve regrowth. The right leg served as the control. The gastrocnemius, soleus, and tibialis (muscles innervated by the sciatic nerve) were collected and used for analysis.

Chemicals. All chemicals were obtained from Sigma-Aldrich (St. Louis, MO) unless otherwise specified.

RESULTS

ROS production is increased in muscle mitochondria during aging and is correlated with muscle atrophy. Our first set of experiments was designed to determine whether the age-related loss of muscle mass is associated with alterations in muscle mitochondrial ROS generation. Atrophy in skeletal muscle as a function of age in C57Bl6 male mice was determined by measuring the mass of a representative muscle, the gastrocnemius. Gastrocnemius muscle mass was reduced nearly 13% at 28 mo in male wild-type mice and >40% at 32 mo compared with 10-mo-old adult control mice (Fig. 1*A*).

ROS production and mitochondrial respiration were measured in muscle mitochondria isolated from 10-, 28-, and 32-mo-old mice. Figure 1*B* shows mitochondrial respiration expressed as the respiratory control ratio (RCR = state 3/state 4 respiration) in mitochondria isolated from muscle of old mice, 28–32 mo of age. The RCR decreased ~33–38% in mitochondria from the older mice.

Measurement of mitochondrial ROS production in isolated mitochondria is most traditionally done in the presence of added substrates, largely because the levels of ROS with endogenous (state 1) substrates are too low to detect. In a previous study, we demonstrated that the fluorogenic probe Amplex red is sensitive enough to detect ROS produced in mitochondria even during state 1, in the absence of exogenous substrates (10). In fact, we previously found that the age-related increase in state 1 ROS generation is greater than in mitochondria exposed to glutamate/malate or succinate as respiratory substrates (55). As shown in Fig. 1*C*, state 1 ROS production was increased nearly twofold in mitochondria isolated from hindlimb skeletal muscle from 28-mo-old male mice compared with mitochondria from 10-mo-old mice. In 32-

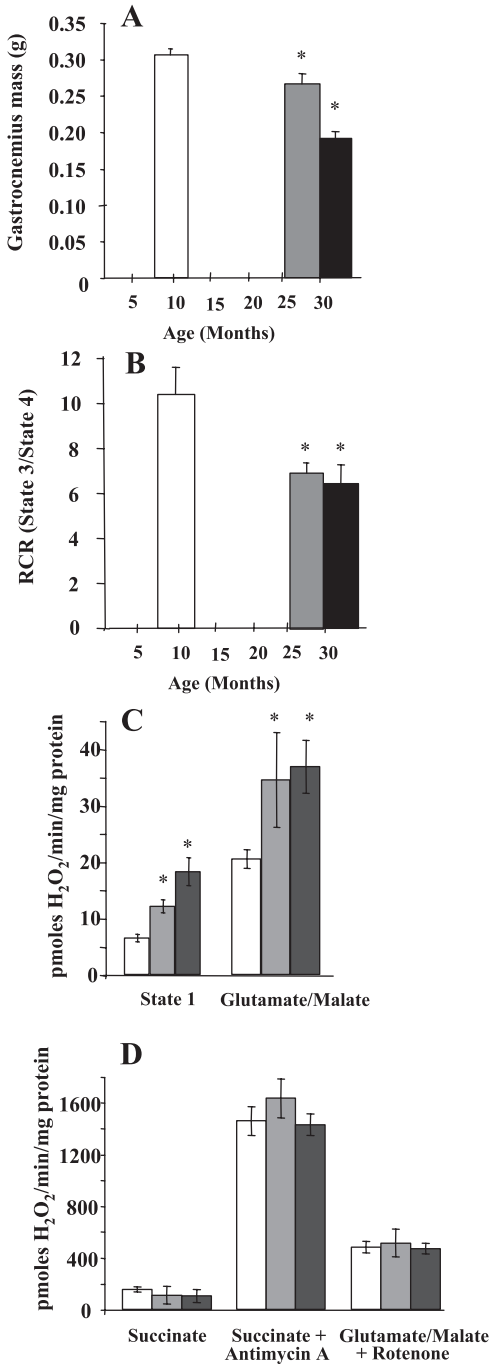

Fig. 1. Increased ROS generation in skeletal muscle mitochondria from young and old mice. Skeletal muscle mitochondria were isolated, and mitochondrial ROS generation was measured as described in EXPERIMENTAL PROCEDURES. The extent of age-related muscle atrophy was assessed by measuring the mass of the gastrocnemius muscle in male wild-type mice at 10, 28, and 32 mo (*A*). *$P < 0.05$, significant difference compared with the 10-mo adult control value (ANOVA with Tukey's post hoc test). *B*: mitochondrial respiration (respiratory control ratio, RCR) measured in the presence of glutamate/malate as respiratory substrate in isolated muscle mitochondria from six 10-mo-old, twelve 28- to 29-mo-old, and eight 32-mo-old mice. *C* and *D*: values are mean (±SE) expressed as rates of mitochondrial ROS release measured in male mice killed at 10 mo (open bars, $n = 6$), 28 mo (light shaded bars, $n = 6$), and 32 mo of age (dark shaded bars, $n = 4$). Values in *C* were measured in the absence of exogenous substrate (state 1) and in the presence of 5 mM glutamate/malate. ROS production in *D* was measured in the presence of 5 mM succinate alone or with the substrates glutamate and malate or succinate in the presence of inhibitors of complex I (rotenone) or complex III (antimycin A). *$P < 0.001$, significant difference from the young wild-type value (ANOVA with Tukey's post hoc test).

mo-old animals, the increase in ROS generation was even greater, reaching levels approximately threefold higher than in 10-mo-old control animals.

Glutamate/malate is a substrate that delivers electrons to complex I of the mitochondrial electron transport chain, after which the electrons are transferred to ubiquinone, complex III, complex IV, and, ultimately, oxygen (59, 69). In mitochondria isolated from muscle of 10-mo-old mice, ROS generation was about five times higher with glutamate/malate than in state 1 without the addition of substrate. ROS generation in mitochondria respiring on glutamate/malate occurs primarily from electron transfer through complex I, but there is also a contribution from complex III (12, 32). ROS production using glutamate/malate was increased with age and was ~40% higher in muscle mitochondria from 28- to 32-mo-old mice compared with mitochondria from 10-mo-old mice (Fig. 1*C*). The difference in ROS production with 5 mM glutamate/malate as a substrate did not reach statistical significance ($P < 0.06$ by ANOVA) when the aged (28 and 32 mo old) animals were treated as independent groups but did reach significance when the aged animals were combined ($P < 0.001$ by ANOVA). When ROS generation with glutamate/malate was stimulated by the addition of the complex I inhibitor rotenone, the rate of ROS generation was increased ~10-fold, but any effect of age disappeared (Fig. 1*D*).

ROS release with the substrate succinate exhibited quite different trends from the results we obtained for state 1 and with glutamate/malate. Most studies indicate the highest rates of H_2O_2 release in isolated mitochondria are obtained with succinate as substrate (32, 80). H_2O_2 released under these conditions is derived from superoxide produced largely during reverse electron transfer through complex I (32, 33). Although the exact physiological significance of this phenomenon is unclear (2, 37), there is considerable interest in succinate-driven reverse electron transfer because this source of ROS is so much greater than any others, at least under conventional conditions (see discussion in Ref. 32) and in the absence of respiratory inhibitors (32, 80). We compared the rates of ROS generation in young and old skeletal muscle mitochondria with succinate as a substrate (Fig. 1*D*) and found that there was no significant change with age, which is in general agreement with other studies that have investigated this question using similar methodology and conditions (32). The addition of antimycin A, the complex III inhibitor, resulted in a seven- to eightfold increase in ROS generation that, similar to the production of ROS in response to the complex I inhibitor rotenone, was not different with age.

Skeletal muscle mitochondrial ROS production is increased in Sod1 null mice and is associated with the degree of muscle atrophy. In agreement with our previous report on *Sod1*$^{-/-}$ mice (57), the gastrocnemius mass was significantly decreased in both young (5 mo) and older (20 mo) *Sod1*$^{-/-}$ mice compared with the age-matched wild-type mice (Fig. 2*A*). At 5 mo, the mass of the gastrocnemius was ~25% lower than in wild-type mice. At 20 mo, the reduction in mass reaches ~50%. The wild-type mice did not show any age-related loss in muscle mass between ages 5 and 20 mo. As shown in Fig. 2*B*, the RCR was decreased ~36% in mitochondria isolated from muscle of 20-mo-old *Sod1*$^{-/-}$ mice compared with mitochondria from muscle of age-matched wild-type mice.

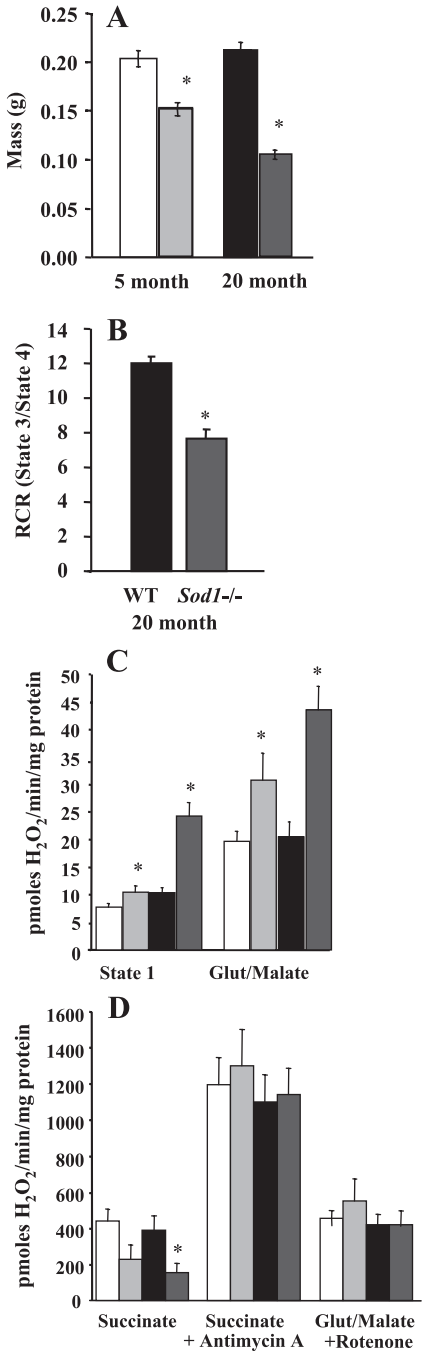

Fig. 2. Increased ROS generation in skeletal muscle mitochondria from *Sod1*$^{-/-}$ mice. *A*: mass of gastrocnemius muscle isolated from female wild-type (WT) and *Sod1*$^{-/-}$ mice at 5 and 20 mo of age. *B*: mitochondrial respiration (RCR) measured in the presence of glutamate/malate as respiratory substrate in isolated muscle mitochondria from 8 WT and 8 *Sod1*$^{-/-}$ mice at 20 mo of age. *$P < 0.05$ significant difference compared with 10-mo-old mice. In *A–D*, open bars represent 5-mo-old WT, light shaded bars represent 5-mo-old *Sod1*$^{-/-}$, dark shaded bars represent 20-mo-old WT, and solid bars represent 20-mo-old *Sod1*$^{-/-}$. *C* and *D*: ROS generation from skeletal muscle mitochondria isolated from the hindlimb of the same group of mice. Values in *C* are means ± SE for state 1 and glutamate (Glut)/malate-supported ROS generation in mitochondria from 5-mo-old WT ($n = 21$) and *Sod1*$^{-/-}$ mice ($n = 10$) and 20-mo-old WT ($n = 16$) and old *Sod1*$^{-/-}$ mice ($n = 16$); values in *D* are means ± SE for ROS generation in the presence of succinate alone, antimycin A+succinate, or glutamate/malate+rotenone. *$P < 0.05$, significant difference in H_2O_2 release in muscle mitochondria from *Sod1*$^{-/-}$ mice compared with mitochondria from age-matched WT mice (ANOVA with Tukey's post hoc test).

State 1 ROS production was increased over 30% in mitochondria from *Sod1*$^{-/-}$ mice at as early as 5 mo of age compared with age-matched wild-type mice (Fig. 2*C*). By 20 mo of age, ROS production in mitochondria from *Sod1*$^{-/-}$ mice was threefold higher than in the age-matched wild-type mice. In mitochondria incubated with glutamate malate as respiratory substrates, ROS release was increased ~35% (30.89 ± 4.77 pmol $H_2O_2 \cdot min^{-1} \cdot mg\ protein^{-1}$ in mitochondria from 5-mo-old *Sod1*$^{-/-}$ compared with 19.77 ± 1.78 pmol $H_2O_2 \cdot min^{-1} \cdot mg\ protein^{-1}$ in age-matched wild-type mice). In 20-mo-old *Sod1*$^{-/-}$ mice, the increase in ROS generation with the substrates glutamate and malate was >100% (Fig. 2*C*). There was no significant difference in ROS production in state 1 or in response to glutamate/malate in mitochondria from the 20-mo-old mice in either group compared with the 5 -mo-old mice (Fig. 2*C*). This is consistent with increased ROS being specifically associated with age-associated muscle loss, since wild-type mice do not show any muscle mass loss at 20 mo compared with the muscle mass at 5 mo of age.

Somewhat unexpectedly, we found that mitochondrial H_2O_2 release with the substrate succinate was significantly lower in mitochondria from the *Sod1*$^{-/-}$ mice compared with wild-type controls, especially in mitochondria from the 20-mo-old *Sod1*$^{-/-}$ mice (Fig. 2*D*). In mitochondria treated with glutamate/malate and the complex I inhibitor rotenone or with succinate and the complex III inhibitor antimycin A, there was no difference between ages and genotypes (Fig. 2*D*).

ROS production is increased in muscle mitochondria in mouse models of ALS and is correlated with the extent of muscle atrophy. We next measured state 1 ROS production in mitochondria in another mouse model associated with significant muscle atrophy, mice expressing mutant forms of CuZn-SOD. We studied two different ALS mutant models, the well-characterized G93A mutant (31) and mice generated using a metal-deficient H46RH48Q mutant (81) that has no CuZn-SOD activity. As shown in Fig. 3, these models had very different patterns of loss of muscle mass during the progression of the disease. The muscle mass of the hindlimb began to decrease as early as 60–70 days in the G93A mutants, even before visible symptoms occurred at the age of onset (Fig. 3, *A* and *C*). However, in the H46RH48Q mutant mice, the hindlimb mass remained essentially unchanged until very late in the disease (Fig. 3, *B* and *D*). Even at the end stage of the disease (shortly before death), hindlimb mass was decreased ~45% in H46RH48Q mice, which is comparable to what is observed in the early stages of the disease in the G93A mutants and in the 20-mo-old (late stage) *Sod1*$^{-/-}$ mice. In contrast, late-stage G93A mice exhibited decreases in hindlimb mass approaching 80%.

The pattern of muscle atrophy correlated closely with increases in mitochondrial ROS production. State 1 ROS release during the disease course in G93A mice was increased almost 10-fold above levels in the mitochondria from wild-type mice, much higher than in the *Sod1*$^{-/-}$ mice or in old wild-type mice, which had relatively less muscle atrophy. In the H46RH48Q mutant mice, there was an up to fourfold increase in ROS release at late stage but virtually no change at early symptomatic stage. In symptomatic stage G93A mice, with glutamate/malate as respiratory substrate, ROS release was increased over sixfold (Fig. 4, *A* and *E*), but in contrast, in the

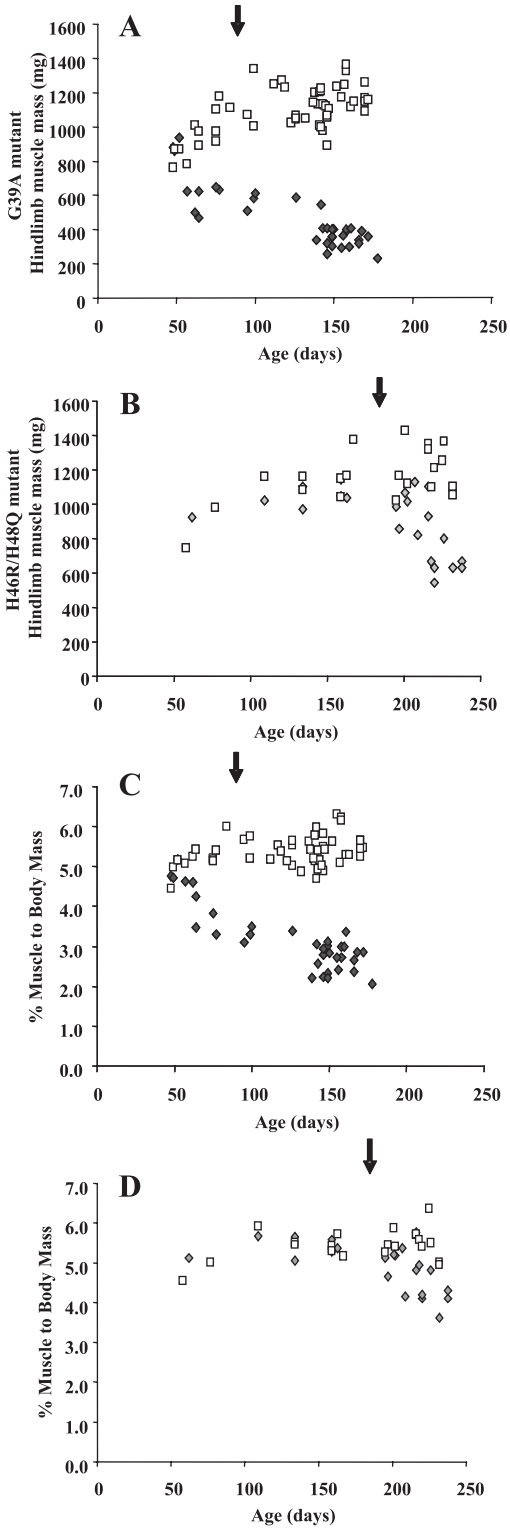

Fig. 3. Muscle mass loss during amyotrophic lateral sclerosis (ALS) in the G93A and H46RH48Q mice. Hindlimb muscle from female G93A (*A*; solid diamonds) or H46RH48Q (*B*; shaded diamonds) as well as nontransgenic, wild-type control mice (open squares) was collected at the ages indicated, and the mass is expressed in mg (*A* and *B*) or relative to body mass (*C* and *D*). Arrows denote the onset of the disease in each mutant.

H46RH48Q mice, ROS release was only ~75% higher compared with the age-matched wild-type control (Fig. 4, *D* and *E*). As we had observed in mitochondria from the *Sod1*$^{-/-}$ mice, ROS production with succinate as a substrate was lower in G93A skeletal muscle mitochondria than in mitochondria from control mice and showed an even greater decrease than had been observed in the *Sod1*$^{-/-}$ mice, approaching levels close to that measured in state 1 in the absence of substrate. As shown in Fig. 4*C*, in addition to the increase in ROS, the RCR was decreased 46% in mitochondria isolated from muscle of end-stage G93A mice compared with age-matched wild-type mice.

ROS production is increased in muscle mitochondria following surgical denervation. To determine whether denervation might be a factor in the increase in mitochondrial ROS in the three models of muscle atrophy studied here, we measured mitochondrial state 1 ROS generation in the gastrocnemius and tibialis anterior muscles following denervation by surgical sciatic nerve transection. ROS release was increased dramatically 5 days after sciatic nerve transection (Fig. 5*A*). As shown in Fig. 5*B*, at 7 days postdenervation, the loss of muscle mass was minimal, yet state 1 ROS production was nearly 30-fold higher in mitochondria isolated from the muscle in the denervated limb compared with the contralateral control limb. ROS release with glutamate/malate was 11-fold higher in the muscle mitochondria from the denervated limb compared with the control limb at 7 days (Fig. 5*C*). There was no significant difference in the rates of ROS production in response to denervation with the use of succinate or in the presence of the inhibitors antimycin A and rotenone (data not shown). The RCR was decreased almost 30% in mitochondria isolated from the muscle in the denervated limb compared with the contralateral control limb (Fig. 5*D*).

The relationship between muscle atrophy and induction of ROS generation by skeletal muscle mitochondria isolated from young and old wild-type mice, 20-mo-old *Sod1*$^{-/-}$ mice, and the two ALS mouse models is illustrated in Fig. 6. The plot clearly shows that models with a greater loss of muscle mass show relatively higher levels of ROS production.

DISCUSSION

The major finding of this study is that ROS production was elevated in skeletal muscle mitochondria isolated from mice representing three different conditions associated with significant loss of muscle mass: age-related muscle atrophy, *Sod1*$^{-/-}$ mice (a mouse model of accelerated sarcopenia), and two ALS mutant mouse models differing in the time course and extent of muscle mass loss during the progression of the disease. Thus, as Fig. 6 illustrates, ROS production was lowest during normal aging (when the extent of muscle atrophy is lowest), higher in muscle from the *Sod1*$^{-/-}$ mice, and increased nearly 10-fold in G93A ALS mutant mice, which showed the most dramatic muscle atrophy. This relationship also holds within each of the models studied, i.e., both ROS production and loss of muscle mass were higher in 32-mo-old than in 27-mo-old normal mice; ROS production and atrophy were higher in 20-mo-old than in 5-mo-old *Sod1*$^{-/-}$ mice; and ROS generation was higher in the G93A compared with the H46RH48Q mutant ALS models and in agreement with more atrophy in G93A.

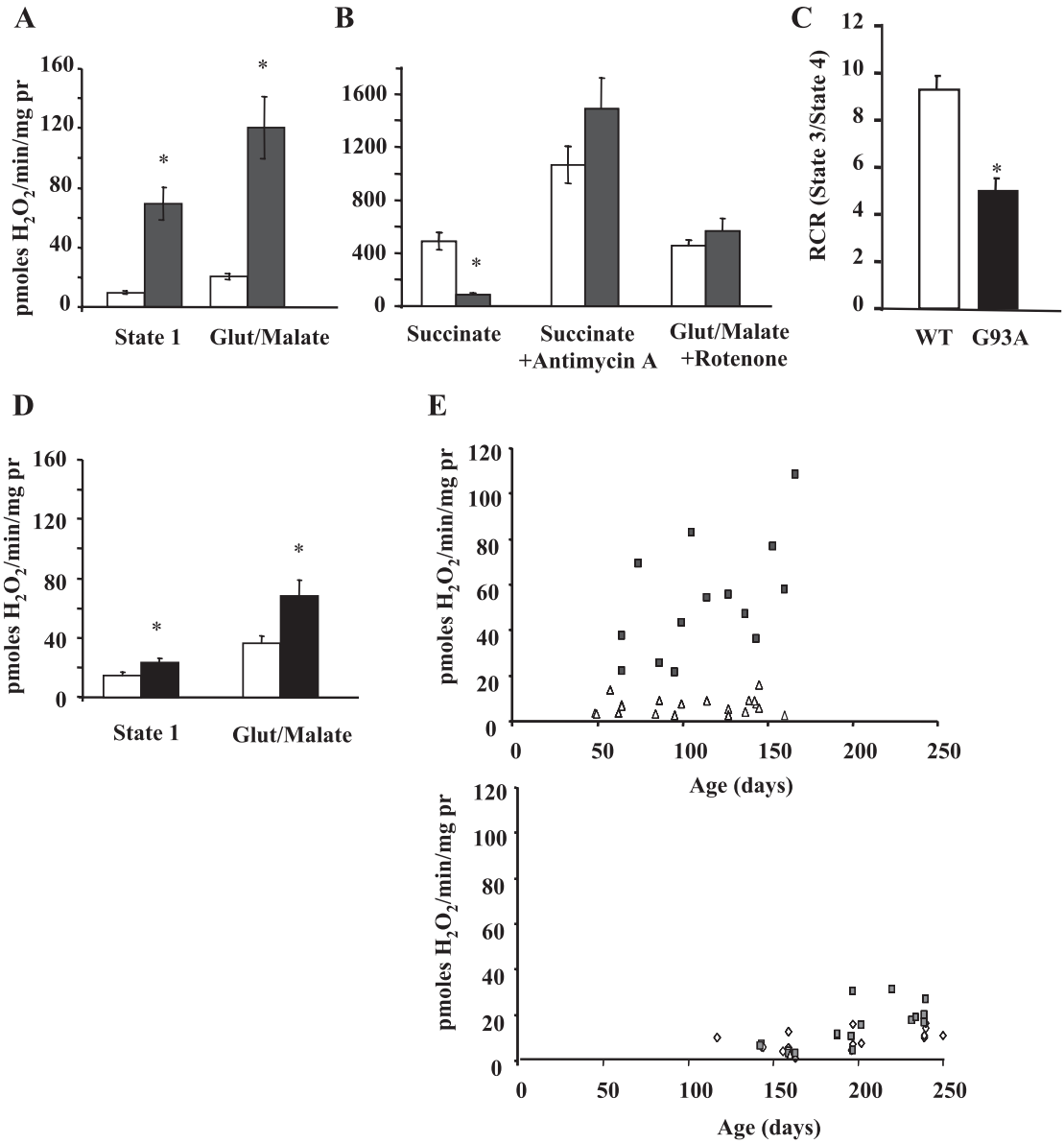

Fig. 4. Increased ROS generation in skeletal muscle mitochondria isolated from ALS transgenic mice. ROS production was measured in skeletal muscle mitochondria of female ALS transgenic mouse models G93A (*A* and *B*) and H46R/H48Q (*D*). Values in *A* and *B* are means ± SE for 12 wild-type control and age-matched G93A transgenic mice (100–140 days of age); values in *D* are means ± SE for 5 wild-type control and age-matched H46R/H48Q mice (200–240 days of age). *$P < 0.001$, significant difference in H_2O_2 release from control in state 1 or with glutamate/malate as substrates (ANOVA). *C*: mitochondrial respiration (RCR) measured in the presence of glutamate/malate as respiratory substrate in isolated muscle mitochondria from 10 wild-type and 10 end-stage G93A mice. *E*: time course of H_2O_2 generation in state 1. ROS production was measured in mitochondria isolated from hindlimb muscle of G93A (*top*) or H46RH48Q transgenic mice (*bottom*) and wild-type littermates at various stages during the life span of the mice. Filled symbols are values measured in mitochondria isolated from G93A and H46RH48Q mice; open triangles and open diamonds denote values measured in wild-type (nontransgenic) mice used as controls for the G93A and H46RH48Q mice, respectively. Note the difference in magnitude of the response.

Each of these three conditions has previously been reported to involve alterations in innervation of skeletal muscle. Innervation is critical for growth and maintenance of muscle fibers, and denervation is well known to cause muscle atrophy (36). Denervation is extensively documented in ALS, caused by the degeneration of lower motor neurons (75), whereas independent lines of evidence also attest to denervation (caused by breakdown of neuromuscular junctions) in *Sod1*$^{-/-}$ mice (25, 57, 70). With respect to aging, it is understood that sarcopenia is a multifactorial process and that denervation plays a significant role (15, 23). During normal aging, there is a loss of motor neurons in the spinal cord and a breakdown of neuromuscular junctions, and axonal sprouting is also impaired (22, 78). Thus one common characteristic of the three models (aging, *Sod1*$^{-/-}$ mice, and ALS mutant mice) is alterations in innervation of muscle fibers (8, 24–26, 41, 67, 70). To test whether denervation contributes to an increase in mitochondrial ROS, we measured ROS generation in mouse muscle following sciatic nerve transection. ROS generation was dramatically increased in surgically denervated muscle, demonstrating a direct role for denervation in increased muscle mitochondrial ROS production. Thus an elevation in ROS

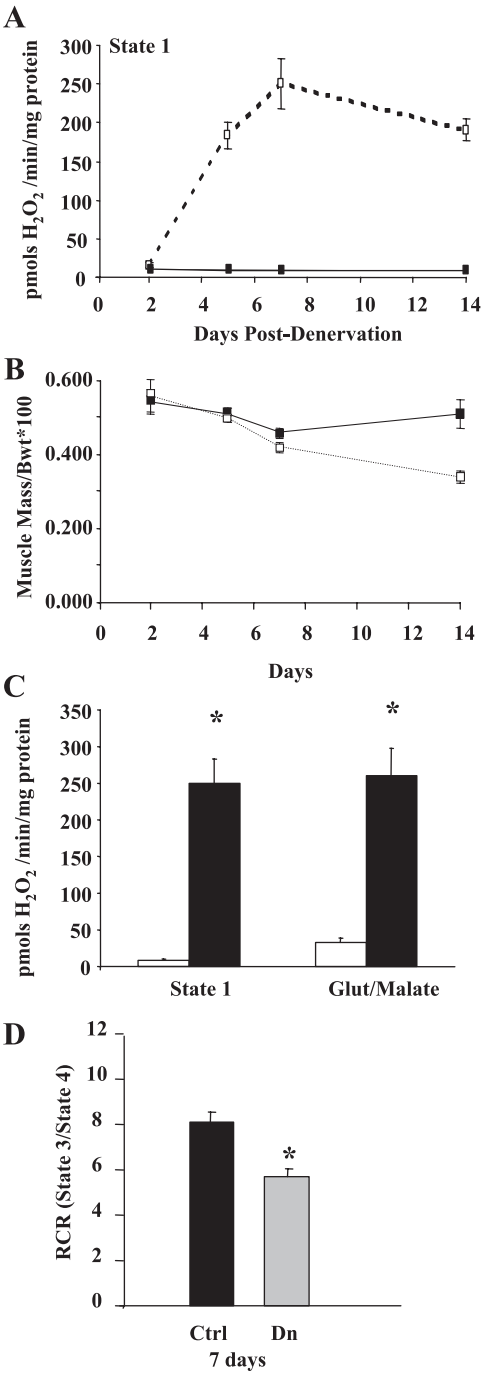

Fig. 5. ROS production is dramatically increased following surgical denervation. Denervation was introduced by surgical transection of the sciatic nerve at the level of the upper femur. The contralateral limb served as a control. Mice were killed, tissues were harvested, and ROS production was measured in isolated muscle mitochondria at 2 ($n = 4$), 5 ($n = 5$), 7 ($n = 6$), and 14 days ($n = 8$) after surgery. *A*: time course of the rate of ROS production in state 1 following denervation (filled squares, denervated muscle). *B*: time course of muscle mass loss, measured as a ratio of weight of the gastrocnemius from the denervated and control legs to body weight (Bwt). *C*: ROS generation in mitochondria from the control (open bars) and denervated muscle (filled bars) 7 days after denervation. Values in *C* are means ± SE for $n = 5$ mice. $^*P < 0.05$, significant difference in ROS generation in muscle mitochondria following denervation compared with mitochondria from control muscle (ANOVA with Tukey's post hoc test). *D*: mitochondrial respiration (RCR) measured in the presence of glutamate/malate as respiratory substrate in isolated muscle mitochondria from 28 wild-type mice 7 days after sciatic nerve transection (Dn). $^*P < 0.05$ by Student's *t*-test.

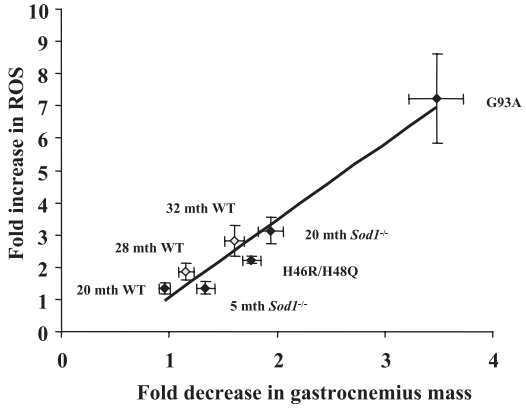

Fig. 6. Correlation between muscle atrophy and ROS production. ROS production data in state 1 are plotted vs. gastrocnemius muscle mass. Muscle mass and ROS production are expressed as the increase relative to young wild-type control values. All values with the exception of the 28- and 32-mo-old wild type represent data collected in female mice. Because the mass of the gastrocnemius is always higher in males, the data from the 28- and 32-mo-old male mice are represented as open symbols. Mth, month.

generation is a common event in skeletal muscle mitochondria under a variety of pathological conditions associated with denervation-induced muscle atrophy.

What is the connection between denervation and altered mitochondrial ROS generation? One potential factor may be a loss of trophic support to the muscle following denervation. Motor neurons are known to exert a trophic effect on skeletal muscle, and in the absence of neural activity, muscle mass decreases, along with a reduction in specific force, fiber diameter, and fiber number (6, 73). Loss of motor neurons, breakdown of neuromuscular junctions, or inhibition of neural signaling occurs in many neuromuscular diseases, including ALS or spinal cord injury (75), spinal muscular atrophy (56), diabetic neuropathy (72), and aging (6, 41, 48), and each of these situations is associated with muscle atrophy. It is possible that lack of trophic factors could have a negative impact on muscle mitochondrial function. Another potential factor linking altered mitochondrial function and denervation is altered calcium handling. Denervation decreases calcium retention capacity in muscle mitochondria, resulting in an overall increase in calcium content in both mitochondria and whole muscle (14). Calcium is a key inducer of the permeability transition pore that regulates mitochondria-mediated cell death; therefore, altered regulation of calcium following denervation can lead to induction of denervation-induced atrophy (71, 74). It is important to consider that although the initiating event is likely a loss of innervation that leads to muscle mitochondrial dysfunction, increased ROS generation, and an increase in oxidative stress, the consequences of these events may produce a positive feedback of oxidative damage that, in turn, damages additional neurons or neuromuscular junctions, exacerbating the increase in muscle ROS generation even further and continuing the cycle of damage.

Mitochondrial alterations have been reported in previous studies using sciatic nerve crush or nerve transection in rodents (1, 38, 39). For example, genes encoding the mitochondrial respiratory chain and the TCA cycle are significantly downregulated following denervation (48, 60, 66), and the levels of cytochrome *c* oxidase, succinate dehydrogenase, citrate syn-

thase, and cardiolipin are significantly lowered 8–14 days after denervation (18, 82). Furthermore, as mentioned above, mitochondria may play a role in muscle atrophy through induction of apoptosis in response to denervation (71). A recent study in rats subjected to nerve transaction also reported an increase in mitochondrial ROS generation that was associated with an increase in the mitochondrial permeability transition and increased apoptosis (1). Together, these studies point to mitochondrial dysfunction following denervation.

How might the increase in mitochondrial ROS production contribute to the loss of muscle mass? Growing evidence implicates oxidative stress as an important regulator of pathways leading to muscle atrophy (27, 36, 65). We can propose several ways that mitochondrial ROS generation might contribute to muscle atrophy. It is possible that the increased in ROS directly or indirectly damages proteins, increasing their turnover, which could contribute to the increase in protein turnover observed after denervation. Alternatively, increased ROS may damage critical enzymes, such as those involved in energy metabolism (45, 51). In fact, increased ROS production following denervation is mirrored by decreases in surface hydrophobicity and enzymatic activity of glyceraldehyde-3-phosphate dehydrogenase and creatine kinase (64), possibly due to increased oxidative damage (63). Increased mitochondrial ROS may also play a signaling role. Another good candidate for an effect of ROS on signaling is NF-κB. NF-κB is known to play a role in muscle atrophy (7, 42), and it is well established that its transcriptional activity can be modulated by H_2O_2 (84). Mitochondria are known to play a central role in intrinsic pathway of apoptosis, and mitochondrial ROS generation and atrophy could also be linked through apoptosis (1, 29, 40). Mitochondrial ROS has also been shown to lead to upregulation of the expression of ubiquitin ligase, Atrogin-1/MAFbx (53), and could therefore contribute to atrophy through increased degradation of proteins by the 26S proteasome system.

One question that arises is whether the loss of innervation precedes the increase in mitochondrial ROS generation or vice versa. Based on our experiments in young and old wild-type mice, the *Sod1*$^{-/-}$ model, and the ALS mouse models, we cannot be certain whether the increase in ROS generation precedes or follows changes in innervation, especially in the *Sod1*$^{-/-}$ mice and in the case of aging, in which the changes occur over a very long time frame (months). What is clear, however, is that in each situation, both muscle atrophy and ROS production increase over time. In ALS mice, muscle atrophy occurs over weeks rather than months, and in this case it is possible to at least roughly correlate the timing of loss of muscle mass and ROS increase. In fact, it has been previously reported that denervation begins as early as 30–40 days of age in G93A ALS mice (24). At this early phase of the disease, we had already detected a small but significant increase in ROS production, supporting the fact that denervation and muscle ROS generation are closely related and suggesting denervation precedes the increase in ROS. Overall, our denervation experiments provide the strongest evidence regarding this issue. ROS generation was significantly increased 2 days after nerve transaction but not at 2 days posttransection. This is strong evidence that the loss of innervation precedes the increase in muscle mitochondrial ROS generation. Furthermore, the sciatic nerve transection demonstrated that an elevation in ROS generation precedes a significant loss in muscle mass (by a few days or so). Although ROS production was increased as early as 5 days after sciatic nerve transection, loss of muscle mass was evident at 7 days. The fact that dramatic changes in ROS were present before the loss of muscle mass supports the hypothesis that ROS may in fact contribute to muscle mass loss.

We unexpectedly found that the degree and dynamics of muscle mass loss were quite different in these two ALS animal models and that these changes correlated with muscle mitochondrial ROS generation. Whereas denervation and muscle mass loss in the G93A mice was evident even before the onset of symptoms (24, 26) (in full agreement with our data in Fig. 4), in the H46RH48Q mice, the extent of muscle mass loss was not only lower but also occurred very late in the disease course (Fig. 4). In effect, the H46RH48Q mice developed ALS despite remarkably little muscle mass loss. Incidentally, ALS patients with the H46R mutation have a very long survival (4). The different patterns of muscle atrophy in the G93A and H46RH48Q mutants provide insight into the role of denervation in the etiology of ALS. ALS has been proposed to be more than a strict neuropathy, that is, skeletal muscle pathology might play an integral part in the disease (16, 17, 54). A converging line of argument suggests that ALS is a distal axonopathy (24), that is, the disease starts at the neuromuscular junction and follows a dying-back pattern. The view that peripheral degeneration is central to the disease is gaining more widespread acceptance (28). However, virtually all of these observations were made in the G93A mice. The fact that H46RH48Q mice develop ALS with only mild muscle mass loss (and that occurs after disease onset) indicates that denervation is unlikely to be a major factor in disease etiology. Although resolving these argument is beyond the scope of this report, the relevant point remains that muscle mass loss is considerably less in the H46RH48Q compared with the G93A mice, which is reflected in the extent of the elevation of ROS production.

Another interesting observation from our experiments is the finding that whereas muscle atrophy was associated with significant increases in mitochondrial ROS production in state 1 and with the substrates glutamate and malate, the exact opposite occurred with the substrate succinate; succinate-supported ROS release was significantly decreased in conditions in which the loss of muscle mass and loss of innervation were significant. For example, although there was no statistically significant difference in succinate-supported ROS release with age, succinate-supported H_2O_2 release was in fact lower in old *Sod1*$^{-/-}$ and late-stage G93A ALS skeletal muscle mitochondria, conditions that are associated with losses in muscle mass >50%. The mechanism(s) driving this decrease in ROS production and the potential physiological relevance of this phenomenon are not clear at this time. H_2O_2 formation with succinate is mostly due to reverse electron transfer through complex I (13, 33, 50), and the physiological relevance of reverse electron transfer is not certain. It has been suggested that succinate-driven reverse electron transfer is likely an isolation artifact that only occurs at concentrations of succinate that are far higher than those found under normal in vivo conditions (32). We therefore conclude that the increases in ROS observed in state 1 that occurred in the presence of

endogenous substrate and with glutamate/malate represent the more physiologically relevant situations.

In summary, we report for the first time that several conditions associated with muscle atrophy and loss of innervation are associated with dramatic increases in mitochondrial production of ROS. Further studies are needed to determine the nature of the link between loss of innervation and mitochondrial dysfunction and the downstream targets and effects of the increase in mitochondrial ROS. A better of understanding of how these factors interact may be instrumental in leading to discovery and use of therapeutic interventions to delay or prevent muscle atrophy associated with alterations in neuromuscular interaction.

ACKNOWLEDGMENTS

We are thankful for the expert technical assistance of Amanda Jernigan and Jay Cox and the editing expertise of Corinne Price.

Present address of W. Song: Dept. of Physical Education, Seoul National University, Seoul, Korea.

GRANTS

Financial support was provided by National Institute on Aging Training Grant 5T3-AG021890-02 (to F. L. Muller), P01 AG20591 (to H. Van Remmen and A. Richardson), Muscular Dystrophy Association Grant MDA3879 (to H. Van Remmen), and a Department of Veterans Affairs MERIT Grant (to H. Van Remmen).

REFERENCES

1. **Adhihetty PJ, O'Leary MF, Chabi B, Wicks KL, Hood DA.** Effect of denervation on mitochondrially mediated apoptosis in skeletal muscle. *J Appl Physiol* 102: 1143–1151, 2007.
2. **Andreyev AY, Kushnareva YE, Starkov AA.** Mitochondrial metabolism of reactive oxygen species. *Biochemistry (Mosc)* 70: 200–214, 2005.
3. **Appell HJ, Duarte JA, Soares JM.** Supplementation of vitamin E may attenuate skeletal muscle immobilization atrophy. *Int J Sports Med* 18: 157–160, 1997.
4. **Arisato T, Okubo R, Arata H, Abe K, Fukada K, Sakoda S, Shimizu A, Qin XH, Izumo S, Osame M, Nakagawa M.** Clinical and pathological studies of familial amyotrophic lateral sclerosis (FALS) with SOD1 H46R mutation in large Japanese families. *Acta Neuropathol (Berl)* 106: 561–568, 2003.
5. **Bielski BHJ.** Reactivity of $HO_2\cdot/O_2^{\cdot-}$ radicals in aqueous solution. *J Phys Chem Ref Data* 14: 1041–1091, 1985.
6. **Brooks SV, Faulkner JA.** Skeletal muscle weakness in old age: underlying mechanisms. *Med Sci Sports Exerc* 26: 432–439, 1994.
7. **Cai D, Frantz JD, Tawa NE Jr, Melendez PA, Oh BC, Lidov HG, Hasselgren PO, Frontera WR, Lee J, Glass DJ, Shoelson SE.** IKKβ/NF-κB activation causes severe muscle wasting in mice. *Cell* 119: 285–298, 2004.
8. **Cardasis CA, LaFontaine DM.** Aging rat neuromuscular junctions: a morphometric study of cholinesterase-stained whole mounts and ultrastructure. *Muscle Nerve* 10: 200–213, 1987.
9. **Chance B, Williams GR.** The respiratory chain and oxidative phosphorylation. *Adv Enzymol Relat Subj Biochem* 17: 65–134, 1956.
10. **Chance B, Williams GR.** A simple and rapid assay of oxidative phosphorylation. *Nature* 175: 1120–1121, 1955.
11. **Chappell JB, Perry SV.** Biochemical and osmotic properties of skeletal muscle mitochondria. *Nature* 173: 1094–1095, 1954.
12. **Chen Q, Vazquez EJ, Moghaddas S, Hoppel CL, Lesnefsky EJ.** Production of reactive oxygen species by mitochondria: central role of complex III. *J Biol Chem* 278: 36027–36031, 2003.
13. **Cino M, Del Maestro RF.** Generation of hydrogen peroxide by brain mitochondria: the effect of reoxygenation following postdecapitative ischemia. *Arch Biochem Biophys* 269: 623–638, 1989.
14. **Csukly K, Ascah A, Matas J, Gardiner PF, Fontaine E, Burelle Y.** Muscle denervation promotes opening of the permeability transition pore and increases the expression of cyclophilin D. *J Physiol* 574: 319–327, 2006.
15. **Delbono O.** Neural control of aging skeletal muscle. *Aging Cell* 2: 21–29, 2003.
16. **Dupuis L, Di Scala F, Rene F, De Tapia M, Oudart H, Pradat PF, Meininger V, Loeffler JP.** Up-regulation of mitochondrial uncoupling protein 3 reveals an early muscular metabolic defect in amyotrophic lateral sclerosis. *FASEB J* 17: 2091–2093, 2003.
17. **Dupuis L, Oudart H, Rene F, Gonzalez de Aguilar JL, Loeffler JP.** Evidence for defective energy homeostasis in amyotrophic lateral sclerosis: benefit of a high-energy diet in a transgenic mouse model. *Proc Natl Acad Sci USA* 101: 11159–11164, 2004.
18. **Eisenberg HA, Hood DA.** Blood flow, mitochondria, and performance in skeletal muscle after denervation and reinnervation. *J Appl Physiol* 76: 859–866, 1994.
19. **Elchuri S, Oberley TD, Qi W, Eisenstein RS, Jackson Roberts L, Van Remmen H, Epstein CJ, Huang TT.** CuZnSOD deficiency leads to persistent and widespread oxidative damage and hepatocarcinogenesis later in life. *Oncogene* 24: 367–380, 2005.
20. **Ernster L, Nordenbrand K.** Skeletal muscle mitochondria. *Methods Enzymol* 10: 86–94, 1967.
21. **Estabrook RW.** Mitochondrial respiratory control and the polarographic measurement of ADP:O ratios. *Methods Enzymol* 10: 41–47, 1974.
22. **Fagg GE, Scheff SW, Cotman CW.** Axonal sprouting at the neuromuscular junction of adult and aged rats. *Exp Neurol* 74: 847–854, 1981.
23. **Faulkner JA, Brooks SV.** Muscle fatigue in old animals. Unique aspects of fatigue in elderly humans. *Adv Exp Med Biol* 384: 471–480, 1995.
24. **Fischer LR, Culver DG, Tennant P, Davis AA, Wang M, Castellano-Sanchez A, Khan J, Polak MA, Glass JD.** Amyotrophic lateral sclerosis is a distal axonopathy: evidence in mice and man. *Exp Neurol* 185: 232–240, 2004.
25. **Flood DG, Reaume AG, Gruner JA, Hoffman EK, Hirsch JD, Lin YG, Dorfman KS, Scott RW.** Hindlimb motor neurons require Cu/Zn superoxide dismutase for maintenance of neuromuscular junctions. *Am J Pathol* 155: 663–672, 1999.
26. **Frey D, Schneider C, Xu L, Borg J, Spooren W, Caroni P.** Early and selective loss of neuromuscular synapse subtypes with low sprouting competence in motoneuron diseases. *J Neurosci* 20: 2534–2542, 2000.
27. **Fulle S, Protasi F, Di Tano G, Pietrangelo T, Beltramin A, Boncompagni S, Vecchiet L, Fano G.** The contribution of reactive oxygen species to sarcopenia and muscle ageing. *Exp Gerontol* 39: 17–24, 2004.
28. **Gould TW, Buss RR, Vinsant S, Prevette D, Sun W, Knudson CM, Milligan CE, Oppenheim RW.** Complete dissociation of motor neuron death from motor dysfunction by Bax deletion in a mouse model of ALS. *J Neurosci* 26: 8774–8786, 2006.
29. **Green D, Kroemer G.** The central executioners of apoptosis: caspases or mitochondria? *Trends Cell Biol* 8: 267–271, 1998.
30. **Gurney ME.** The use of transgenic mouse models of amyotrophic lateral sclerosis in preclinical drug studies. *J Neurol Sci* 152, *Suppl* 1: S67–S73, 1997.
31. **Gurney ME, Pu H, Chiu AY, Dal Canto MC, Polchow CY, Alexander DD, Caliendo J, Hentati A, Kwon YW, Deng HX, Chen W, Zhai P, Sufit RL, Siddique T.** Motor neuron degeneration in mice that express a human Cu,Zn superoxide dismutase mutation. *Science* 264: 1772–1775, 1994.
32. **Hansford RG, Hogue BA, Mildaziene V.** Dependence of H_2O_2 formation by rat heart mitochondria on substrate availability and donor age. *J Bioenerg Biomembr* 29: 89–95, 1997.
33. **Hinkle PC, Butow RA, Racker E, Chance B.** Partial resolution of the enzymes catalyzing oxidative phosphorylation. XV. Reverse electron transfer in the flavin-cytochrome beta region of the respiratory chain of beef heart submitochondrial particles. *J Biol Chem* 242: 5169–5473, 1967.
34. **Holloszy JO, Chen M, Cartee GD, Young JC.** Skeletal muscle atrophy in old rats: differential changes in the three fiber types. *Mech Ageing Dev* 60: 199–213, 1991.
35. **Huang TT, Yasunami M, Carlson EJ, Gillespie AM, Reaume AG, Hoffman EK, Chan PH, Scott RW, Epstein CJ.** Superoxide-mediated cytotoxicity in superoxide dismutase-deficient fetal fibroblasts. *Arch Biochem Biophys* 344: 424–432, 1997.
36. **Jackman RW, Kandarian SC.** The molecular basis of skeletal muscle atrophy. *Am J Physiol Cell Physiol* 287: C834–C843, 2004.
37. **Jezek P, Hlavata L.** Mitochondria in homeostasis of reactive oxygen species in cell, tissues, and organism. *Int J Biochem Cell Biol* 37: 2478–2503, 2005.
38. **Joffe M, Savage N, Isaacs H.** Biochemical functioning of mitochondria in normal and denervated mammalian skeletal muscle. *Muscle Nerve* 4: 514–519, 1981.

39. **Joffe M, Savage N, Isaacs H.** Increased muscle calcium. A possible cause of mitochondrial dysfunction and cellular necrosis in denervated rat skeletal muscle. *Biochem J* 196: 663–667, 1981.
40. **Joza N, Oudit GY, Brown D, Benit P, Kassiri Z, Vahsen N, Benoit L, Patel MM, Nowikovsky K, Vassault A, Backx PH, Wada T, Kroemer G, Rustin P, Penninger JM.** Muscle-specific loss of apoptosis-inducing factor leads to mitochondrial dysfunction, skeletal muscle atrophy, and dilated cardiomyopathy. *Mol Cell Biol* 25: 10261–10272, 2005.
41. **Kadhiresan VA, Hassett CA, Faulkner JA.** Properties of single motor units in medial gastrocnemius muscles of adult and old rats. *J Physiol* 493: 543–552, 1996.
42. **Kandarian SC, Jackman RW.** Intracellular signaling during skeletal muscle atrophy. *Muscle Nerve* 33: 155–165, 2006.
43. **Karakelides H, Sreekumaran Nair K.** Sarcopenia of aging and its metabolic impact. *Curr Top Dev Biol* 68: 123–148, 2005.
44. **Kettle AJ, Carr AC, Winterbourn CC.** Assays using horseradish peroxidase and phenolic substrates require superoxide dismutase for accurate determination of hydrogen peroxide production by neutrophils. *Free Radic Biol Med* 17: 161–164, 1994.
45. **Knyushko TV, Sharov VS, Williams TD, Schoneich C, Bigelow DJ.** 3-Nitrotyrosine modification of SERCA2a in the aging heart: a distinct signature of the cellular redox environment. *Biochemistry* 44: 13071–13081, 2005.
46. **Kondo H, Miura M, Nakagaki I, Sasaki S, Itokawa Y.** Trace element movement and oxidative stress in skeletal muscle atrophied by immobilization. *Am J Physiol Endocrinol Metab* 262: E583–E590, 1992.
47. **Kostrominova TY, Dow DE, Dennis RG, Miller RA, Faulkner JA.** Comparison of gene expression of 2-mo denervated, 2-mo stimulated-denervated, and control rat skeletal muscles. *Physiol Genomics* 22: 227–243, 2005.
48. **Kostrominova TY, Macpherson PC, Carlson BM, Goldman D.** Regulation of myogenin protein expression in denervated muscles from young and old rats. *Am J Physiol Regul Integr Comp Physiol* 279: R179–R188, 2000.
49. **Krasnoff J, Painter P.** The physiological consequences of bed rest and inactivity. *Adv Ren Replace Ther* 6: 124–132, 1999.
50. **Krishnamoorthy G, Hinkle PC.** Studies on the electron transfer pathway, topography of iron-sulfur centers, and site of coupling in NADH-Q oxidoreductase. *J Biol Chem* 263: 17566–17575, 1988.
51. **Lebherz HG.** Content and synthesis of glycolytic enzymes in normal, denervated, and dystrophic skeletal muscle fibers. *Int J Biochem* 16: 1201–1205, 1984.
52. **Leeuwenburgh C.** Role of apoptosis in sarcopenia. *J Gerontol A Biol Sci Med Sci* 58: 999–1001, 2003.
53. **Li YP, Chen Y, John J, Moylan J, Jin B, Mann DL, Reid MB.** TNF-α acts via p38 MAPK to stimulate expression of the ubiquitin ligase atrogin1/MAFbx in skeletal muscle. *FASEB J* 19: 362–370, 2005.
54. **Mahoney DJ, Kaczor JJ, Bourgeois J, Yasuda N, Tarnopolsky MA.** Oxidative stress and antioxidant enzyme upregulation in SOD1-G93A mouse skeletal muscle. *Muscle Nerve* 33: 809–816, 2006.
55. **Mansouri A, Muller FL, Liu Y, Ng R, Faulkner J, Hamilton M, Richardson A, Huang TT, Epstein CJ, Van Remmen H.** Alterations in mitochondrial function, hydrogen peroxide release and oxidative damage in mouse hind-limb skeletal muscle during aging. *Mech Ageing Dev* 127: 298–306, 2006.
56. **Monani UR.** Spinal muscular atrophy: a deficiency in a ubiquitous protein; a motor neuron-specific disease. *Neuron* 48: 885–896, 2005.
57. **Muller FL, Song W, Liu Y, Chaudhuri A, Pieke-Dahl S, Strong R, Huang TT, Epstein CJ, Roberts LJ 2nd, Csete M, Faulkner JA, Van Remmen H.** Absence of CuZn superoxide dismutase leads to elevated oxidative stress and acceleration of age-dependent skeletal muscle atrophy. *Free Radic Biol Med* 40: 1993–2004, 2006.
58. **Nader GA.** Molecular determinants of skeletal muscle mass: getting the "AKT" together. *Int J Biochem Cell Biol* 37: 1985–1996, 2005.
59. **Nicholls DG, Ferguson SJ.** *Bioenergetics 3*. London: Academic, 2002.
60. **Nikawa T, Ishidoh K, Hirasaka K, Ishihara I, Ikemoto M, Kano M, Kominami E, Nonaka I, Ogawa T, Adams GR, Baldwin KM, Yasui N, Kishi K, Takeda S.** Skeletal muscle gene expression in space-flown rats. *FASEB J* 18: 522–524, 2004.
61. **Oppenheimer EA.** Treating respiratory failure in ALS: the details are becoming clearer. *J Neurol Sci* 209: 1–4, 2003.
62. **Pak JW, Herbst A, Bua E, Gokey N, McKenzie D, Aiken JM.** Mitochondrial DNA mutations as a fundamental mechanism in physiological declines associated with aging. *Aging Cell* 2: 1–7, 2003.
63. **Pierce A, de Waal E, Muller F, Vanremmen H, Richardson A, Chaudhuri A.** Common and unique proteins affected in two FALS animal models: a novel fluorescence-based proteomic approach for measuring irreversible cysteine oxidation. *Free Radic Biol Med* 39: S63–S63, 2005.
64. **Pierce A, deWaal E, VanRemmen H, Richardson A, Chaudhuri A.** A novel approach for screening the proteome for changes in protein conformation. *Biochemistry* 45: 3077–3085, 2006.
65. **Powers SK, Kavazis AN, DeRuisseau KC.** Mechanisms of disuse muscle atrophy: role of oxidative stress. *Am J Physiol Regul Integr Comp Physiol* 288: R337–R344, 2005.
66. **Raffaello A, Laveder P, Romualdi C, Bean C, Toniolo L, Germinario E, Megighian A, Danieli-Betto D, Reggiani C, Lanfranchi G.** Denervation in murine fast-twitch muscle: short-term physiological changes and temporal expression profiling. *Physiol Genomics* 25: 60–74, 2006.
67. **Reaume AG, Elliott JL, Hoffman EK, Kowall NW, Ferrante RJ, Siwek DF, Wilcox HM, Flood DG, Beal MF, Brown RH Jr, Scott RW, Snider WD.** Motor neurons in Cu/Zn superoxide dismutase-deficient mice develop normally but exhibit enhanced cell death after axonal injury. *Nat Genet* 13: 43–47, 1996.
68. **Roubenoff R, Hughes VA.** Sarcopenia: current concepts. *J Gerontol A Biol Sci Med Sci* 55: M716–M724, 2000.
69. **Scheffler IE.** *Mitochondria*. New York: Wiley-Liss, 1999.
70. **Shefner JM, Reaume AG, Flood DG, Scott RW, Kowall NW, Ferrante RJ, Siwek DF, Upton-Rice M, Brown RH Jr.** Mice lacking cytosolic copper/zinc superoxide dismutase display a distinctive motor axonopathy. *Neurology* 53: 1239–1246, 1999.
71. **Siu PM, Alway SE.** Mitochondria-associated apoptotic signalling in denervated rat skeletal muscle. *J Physiol* 565: 309–323, 2005.
72. **Sullivan KA, Feldman EL.** New developments in diabetic neuropathy. *Curr Opin Neurol* 18: 586–590, 2005.
73. **Sunderland S, Ray L.** Denervation changes in mammalian striated muscle. *J Neurol Neurosurg Psychiatry* 13: 159–177, 1950.
74. **Tews DS.** Apoptosis and muscle fibre loss in neuromuscular disorders. *Neuromuscul Disord* 12: 613–622, 2002.
75. **Thomas CK, Zijdewind I.** Fatigue of muscles weakened by death of motoneurons. *Muscle Nerve* 33: 21–41, 2006.
76. **Thomason DB, Booth FW.** Atrophy of the soleus muscle by hindlimb unweighting. *J Appl Physiol* 68: 1–12, 1990.
77. **Tisdale MJ.** Cancer cachexia: metabolic alterations and clinical manifestations. *Nutrition* 13: 1–7, 1997.
78. **Tomlinson BE, Irving D.** The numbers of limb motor neurons in the human lumbosacral cord throughout life. *J Neurol Sci* 34: 213–219, 1977.
79. **Viguie CA, Lu DX, Huang SK, Rengen H, Carlson BM.** Quantitative study of the effects of long-term denervation on the extensor digitorum longus muscle of the rat. *Anat Rec* 248: 346–354, 1997.
80. **Votyakova TV, Reynolds IJ.** $\Delta\Psi_m$-dependent and -independent production of reactive oxygen species by rat brain mitochondria. *J Neurochem* 79: 266–277, 2001.
81. **Wang J, Xu G, Gonzales V, Coonfield M, Fromholt D, Copeland NG, Jenkins NA, Borchelt DR.** Fibrillar inclusions and motor neuron degeneration in transgenic mice expressing superoxide dismutase 1 with a disrupted copper-binding site. *Neurobiol Dis* 10: 128–138, 2002.
82. **Wicks KL, Hood DA.** Mitochondrial adaptations in denervated muscle: relationship to muscle performance. *Am J Physiol Cell Physiol* 260: C841–C850, 1991.
83. **Williams MD, Van Remmen H, Conrad CC, Huang TT, Epstein CJ, Richardson A.** Increased oxidative damage is correlated to altered mitochondrial function in heterozygous manganese superoxide dismutase knockout mice. *J Biol Chem* 273: 28510–28515, 1998.
84. **Zhou LZ, Johnson AP, Rando TA.** NF κB and AP-1 mediate transcriptional responses to oxidative stress in skeletal muscle cells. *Free Radic Biol Med* 31: 1405–1416, 2001.
85. **Zhou M, Diwu Z, Panchuk-Voloshina N, Haugland RP.** A stable nonfluorescent derivative of resorufin for the fluorometric determination of trace hydrogen peroxide: applications in detecting the activity of phagocyte NADPH oxidase and other oxidases. *Anal Biochem* 253: 162–168, 1997.